ACCSCIENCE PUBLISHING

Engineering Science in Additive Manufacturing

ORIGINAL RESEARCH ARTICLE

Three-dimensional (3D) bioprinting of coral-polyp bio-skin using ultrashort and biofunctionalized peptide bioinks for transplantation on coral skeletons

Alexander U. Valle-Pérez[1,2], Manola Moretti[1,2], Panayiotis Bilalis[1,2], Sebastian Overmans[3], Kyle J. Lauersen[3], Christian Baumgartner[4], and Charlotte A. E. Hauser[1,2,4]*

[1]Laboratory for Nanomedicine, Division of Biological and Environmental Science and Engineering (BESE), King Abdullah University of Science and Technology, Thuwal, Mecca Province, Kingdom of Saudi Arabia

[2]Computational Bioscience Research Center (CBRC), King Abdullah University of Science and Technology, Thuwal, Mecca Province, Kingdom of Saudi Arabia

[3]Laboratory for Sustainable & Synthetic Biotechnology, Division of Biological and Environmental Sciences and Engineering (BESE), King Abdullah University of Science and Technology (KAUST), Thuwal, Mecca Province, Kingdom of Saudi Arabia

[4]Institute of Health Care Engineering with European Testing Center of Medical Devices, Graz University of Technology (TU Graz), Graz, Styria, Austria

***Corresponding author:**
Charlotte A.E. Hauser
(charlotte.hauser-funke@tugraz.at)

Citation: Valle-Pérez AU, Moretti M, Bilalis P, *et al.* Three-dimensional (3D) bioprinting of coral-polyp bio-skin using ultrashort and biofunctionalized peptide bioinks for transplantation on coral skeletons. *Eng Sci Add Manuf*. 2025;1(3):025270017. doi: 10.36922/ESAM025270017

Received: July 5, 2025

Revised: August 12, 2025

Accepted: August 19, 2025

Published online: September 18, 2025

Abstract

There is growing interest in applying 3D printing technologies to environmental restoration, particularly for fabricating bio-inspired artificial reefs and printing coral skeletons to attract fish and support coral growth and survival. More recently, tissue engineering and 3D bioprinting strategies have been employed to develop biomimetic biomaterials that more closely replicate the natural coral microenvironment, including the incorporation of coral symbionts, to aid restoration efforts. In this study, we investigate the use of diverse ultrashort peptide- and biofunctionalized peptide-based bioinks to support bail-out polyp re-settlement and subsequent micropropagation. Among the 13 bioinks examined, eight demonstrated polyp biocompatibility and stability under seawater conditions. We focused on two Scleractinia species, *Stylophora pistillata* and *Pocillopora verrucosa*, and optimized a culture strategy for microencapsulated bail-out polyps following re-settlement, comparing a single-entity versus clustered-entity approach. These advancements lay the groundwork for polyp transplantation using biomimetic biomaterials. The top-performing bioinks were selected based on bioink underwater stability, polyp biocompatibility, and suitability for 3D bioprinting of polyps onto coral skeletons. This led to the development of a coral-inspired, polyp-containing bio-skin graft designed to promote coral tissue regeneration. Here, we report the first results demonstrating the use of bioinks for coral polyp microencapsulation and 3D bioprinting with ultrashort peptide-based bioinks to support coral regeneration and transplantation on coral skeletons.

Keywords: 3D bioprinting; Artificial coral tissue; Ultrashort peptide bioinks; Biofunctionalized bioinks; Coral polyp microencapsulation; Coral polyp transplantation; Polyp bail-out

1. Introduction

Corals are crucial organisms within coral reefs, which are among the most biodiverse marine ecosystems, despite covering only about 1% of the ocean floor. The presence and health of corals are key indicators of ecosystem resilience or vulnerability. However, climate change and anthropogenic pressures, such as rising sea surface temperatures and the metabolic costs of growth, place corals at substantial risk. This vulnerability also endangers many associated species. During heat waves and ocean acidification events, corals often expel their symbiotic microalgae, causing coral bleaching. Therefore, there is an urgent need to strengthen coral resilience through both conventional restoration practices and the development of innovative biotechnological approaches.

Corals maintain a symbiotic relationship with zooxanthellae, symbiotic microalgae residing within their tissues, which are responsible for the coral's vivid pigmentation. Through photosynthesis and the metabolism of nitrates and phosphates, these algae provide essential nutrients to their coral hosts. However, corals are highly sensitive to environmental fluctuations, especially abrupt temperature increases. During a heat wave, when water temperatures rise and remain elevated for prolonged periods, this relationship is disrupted, leading to a reduction in the symbiotic microalgae population (coral bleaching). As a result, the coral loses its color, exposing its whitish calcium carbonate skeleton. At this stage, the coral becomes vulnerable to starvation and diseases. While recovery is possible if conditions improve, prolonged stress often leads to mortality. In addition, research has shown that a single coral colony can host multiple species of microalgae.[1,2]

The term "polyp bail-out" refers to the detachment of individual polyps from a coral as a response to environmental stress and as a form of asexual reproduction in certain species, such as reef-building (scleractinian) corals.[3,4] Recently, the bail-out has been used as a model system in coral biology, with single-detached polyps utilized in applications such as the development of polyp-on-chip microfluidic devices for polyp culture and development.[5-7] The bail-out process has been previously described in the literature.[8] One method of inducing bail-out is changing osmolarity to stress the coral, which results in the detachment of individual polyps from the underlying coral skeleton. After bail-out, polyps disperse, settle in new locations, and initiate skeletogenesis and calcification.[3] However, successful re-settlement remains challenging, as only a small proportion of polyps reattach, and many show no signs of settlement even 3 months after bail-out.[4] In addition, the viability of polyps post-bail-out varies depending on the coral species and experimental conditions.[5,8]

The amphiphilic self-assembling peptides used in this study are compounds with both hydrophobic and hydrophilic regions. These peptides assemble into fibers and subsequently into 3D fibrous supramolecular structures in the form of hydrogels via non-covalent interactions. When ionic solutions such as phosphate-buffered saline (PBS) are added to aqueous peptide solutions, fiber formation is accelerated, reducing gelation times to minutes or even seconds, depending on the specific peptide sequence and concentration. For example, peptide-based bioinks B1–B3, employed in the present study and previously reported in other research, gelate within 1–3 min when dissolved in water at a concentration of 10 mg/mL and subsequently mixed with 10× PBS.[9] Thus, gelation time is strongly dependent on peptide concentration. These properties emphasize amphiphilic peptides as ideal bioink materials for extrusion-based 3D bioprinting, allowing for instantaneous layer-by-layer printing of cell-laden constructs.

Furthermore, the attachment of bioactive cellular motifs to ultrashort peptide compounds yields biofunctionalized peptides with enhanced functionality, which can induce cellular responses such as cell adhesion, proliferation, and differentiation. However, these biofunctionalized peptides often exhibit reduced or inhibited self-assembling capabilities. To overcome this limitation, strictly defined ratios of biofunctionalized peptides can be mixed with ultrashort self-assembling peptides, thereby enabling nanofiber and hydrogel formation. This approach results in functional scaffold microenvironments suitable for cell culture and 3D bioprinting applications.

The technique of 3D bioprinting is expected to play a crucial role in future coral reef restoration efforts.[10] This technology has already been widely applied in biomanufacturing human cell-laden organs and tissues, such as skin and cartilage, as well as in the microencapsulation of microalgae-based structures.[11-14] More recently, the integration of 3D bioprinting, bioinks, and biomaterials has been explored for coral restoration.[15,16] Advancements include the 3D printing of microalgal structures using silk/hydroxypropyl methylcellulose ink mixtures, coral propagation through additive manufacturing, the development of bacteria-based materials for coral restoration, bioprinting symbionts to create coral-like skeletons, and the fabrication of microenvironments resembling natural corals, among other applications.[13,14,17-21] Furthermore, biomaterials have been engineered with antioxidants to mitigate coral bleaching and promote coral

cell adhesion.[22,23] Therefore, developing next-generation bioinks and biomaterials incorporating symbiotic microorganisms through biofabrication could significantly enhance ongoing coral restoration efforts. Future research may focus on employing 3D bioprinting and bioinks to accelerate coral tissue regeneration *in situ*.

In the current research, we combined ultrashort peptide-based bioinks, 3D bioprinting, and bail-out polyps to create a coral-inspired bio-skin biomaterial for coral tissue regeneration. Polyps were microencapsulated in 3D scaffolds using various biocompatible bioinks, and their potential for sustaining bail-out polyps and enabling micropropagation was assessed. Two species of bail-out polyps, *Stylophora pistillata* and *Pocillopora verrucosa*, were microencapsulated, and two culture methods were explored: individual units and clustered entities. Eight out of 13 investigated bioinks (Table 1) facilitated polyp re-settlement and supported micropropagation. Polyps cultured as clustered entities formed interconnections, retained their green and red fluorescence, and produced surrounding tissue, all indicative of micropropagation. The viscoelastic properties of the most effective bioinks were subsequently evaluated under seawater conditions to assess their suitability for field applications. After identifying the top-performing bioink in terms of underwater stability and polyp biocompatibility, we optimized a robotic-assisted extrusion-based 3D bioprinting system to create a structurally stable coral bio-skin that supported viable polyps for up to 10 days.

2. Materials and methods

2.1. Peptide synthesis

Thirteen individual ultrashort peptides and biofunctionalized peptide derivatives were synthesized to develop bioinks (Table 1). All synthesized peptides were N-terminally acetylated (Ac–peptide) and C-terminally amidated (peptide–NH_2) to prevent the influence of terminal charges (Ac–peptide–NH_2). The synthesized peptide sequences were as follows: Ac-Ile-Cha-Cha-Lys-NH_2 (IZZK), Ac-Ile-Ile-Cha-Lys-NH_2 (IIZK), Ac-Ile-Ile-Phe-Lys-NH_2 (IIFK), Ac-Phe-Phe-Ile-Lys-NH_2 (FFIK), Ac-Phe-Ile-Ile-Lys-NH_2 (FIIK), Ac-Leu-Ile-Val-Ala-Gly-Lys-NH_2 (LIVAGK), Ac-Ile-Val-Cha-Lys-NH_2 (IVZK), Ac-Ile-Val-Phe-Lys-NH_2 (IVFK), Ac-Ile-Ile-Cha-Lys-Gly-Gly-Gly-Arg-Gly-Asp-Ser-NH_2 (IIZKGGGRGDS), Ac-Ile-Ile-Cha-Lys-Gly-Gly-Gly-Phe-Hyp-Gly-Glu-Arg-NH_2 (IIZKGGGFOGER), Ac-Ile-Ile-Phe-Lys-Gly-Gly-Gly-Tyr-Ile-Gly-Ser-Arg-NH_2 (IIFKGGGYIGSR), Ac-Ile-Ile-Phe-Lys-Gly-Gly-Gly-Arg-Gly-Asp-Ser-NH_2 (IIFKGGGRGDS), and Ac-Ile-Cha-Cha-Glu-NH_2 (IZZE).

Peptides were synthesized using solid-phase peptide synthesis on a CS136X synthesizer (CSBIO, US). After synthesis, peptides were cleaved from the resin using a mixture of 95% trifluoroacetic acid, 2.5% triisopropylsilane, and 2.5% water at room temperature for 2 h. Precipitation was initiated by adding cold diethyl ether to the peptide solution, which was then kept overnight at 4°C. The precipitated peptides were collected by centrifugation and subsequently purified by reverse-phase high-performance

Table 1. Bioink scaffold formulations and stability under seawater conditions

Bioink	Peptide sequence 1	Peptide sequence 2	Mixing ratio	Total final concentration (mg/ml)	Assembled under seawater conditions?	Stability under seawater conditions (days)	Remarks after 30 days in seawater
B1	IIZK	NA	NA	10	Yes	>30	100% of samples remained stable
B2	IZZK	NA	NA		Yes	>30	100% of samples remained stable
B3	IIFK	NA	NA		Yes	>30	100% of samples remained stable
B4	FFIK	NA	NA		Yes	<14	100% of samples dissolved
B5	FIIK	NA	NA		Yes	>30	75% of samples remained stable; partial dissolution observed
B6	LIVAGK	NA	NA		Yes	<24	100% of samples dissolved
B7	IVZK	NA	NA		Yes	>30	75% of samples remained stable; partial dissolution observed
B8	IVFK	NA	NA		Yes	>30	75% of samples remained stable; partial dissolution observed
B9	IIZKGGGRGDS	IIZK	1:1		Yes	>30	75% of samples remained stable; partial dissolution observed
B10	IIZKGGGFOGER	IIZK	1:1		Yes	>30	50% of samples remained stable
B11	IIFKGGGYIGSR	IIFK	2:1		Yes	>30	75% of samples remained stable; partial dissolution observed
B12	IIFKGGGRGDS	IIFK	2:1		Yes	>30	25% of samples remained stable
B13	IZZE	NA	NA		No	0	100% of samples dissolved

liquid chromatography on a C-18 column (2–98% acetonitrile over 15 min) at a flow rate of 20 mL/min, achieving yields of over 60%. Peptides were stored in sealed Falcon containers at −80°C, and peptide aliquots were prepared for experiments. Chemical structures were verified through mass spectrometry.

2.2. Bioink scaffold formation

The ultrashort peptides exhibited self-assembling scaffold capabilities even in the presence of water. Peptide solutions were prepared by dissolving the selected ultrashort peptide powder in 900 µL of ultrapure cell culture-grade water. In contrast, biofunctionalized peptides lacked self-assembling capability and were therefore mixed with ultrashort peptide powder before dissolution. The mixed peptide powders were weighed and dissolved in 900 µL of ultrapure, cell culture-grade water, as described in Table 1. Hydrogel scaffold formation was accelerated by adding PBS at a 1:10 ratio (PBS to peptide solution).

2.3. Polyp bail-out

The coral species *S. pistillata* and *P. verrucosa* were obtained from the Al Fahal reef (22.305118 N; 38.964568 E). Small fragments (1 cm long) were collected and used for polyp extraction through the high-salinity seawater method. The fragments were placed in a container with 3 L of isosmotic seawater connected to a peristaltic pump. High-salinity seawater was then introduced into the container at a flow rate of 126 mL/h for 24 h. This high-salinity seawater was prepared by adding sodium chloride to 3 L of Red Sea water (40 PSU) until a total salinity of 74 PSU was reached. The resulting osmotic stress caused the detachment of individual polyps. Further details on the bail-out methodology can be found in the literature.[5,6]

2.4. Polyp microencapsulation and 3D bioprinting

Peptides and peptide mixtures were prepared at a concentration of 10 mg/mL (w/v) using a 1:10 ratio, as shown in Table 1. Each peptide solution was prepared by dissolving the weighted peptide powder in 900 µL of ultrapure cell culture-grade water. Hydrogel biomaterials were then generated by carefully placing either a single polyp or a cluster of five nearby polyps (not in direct contact) into a 96-well plate containing 135 µL of peptide solution. Immediately after adding the polyp(s), 15 µL of PBS was introduced into each well to initiate microencapsulation. Filtered seawater (FSW; using a 20 µm filter) was subsequently added until the biomaterials were completely submerged. The hydrogels were maintained on a magnetic stirrer with temperature control (IKA® RCT basic, IKA-Werke GmbH & Co. KG, Germany) at 27°C under aquarium lights (Radion XR15 G5 Blue, controlled by the Mobius app including the acclimation feature software, EcoTech Marine, US) with a 12 h light–dark cycle at 50% light intensity.

2.5. Polyp culture

The hydrogel biomaterials were cultured under semi-batch conditions, with FSW replaced every 2 days. A thermometer was used throughout the experiment to monitor and prevent overheating of the system.

2.6. Viscoelastic characterization

Hydrogels were prepared by mixing 135 µL of peptide solution with 15 µL of PBS inside a 9 mm internal-diameter glass ring. FSW was then added until the hydrogels were fully covered. After 12 h, the glass rings were removed, and the samples were monitored for 30 days. The viscoelastic properties of the peptide hydrogels – including stiffness, viscosity, and thixotropy – were analyzed using an Ares-G2 Rheometer (TA Instruments, US) equipped with an advanced Peltier system (Waters, TA Instruments, APS, US). Stiffness was measured using an 8 mm parallel plate with a 1.5 mm gap between the upper and lower plates. Three consecutive tests were performed:

- Time-sweep: 5 min at an angular frequency of 1 rad/s and a strain of 0.1%.
- Frequency-sweep: 0.1–100 rad/s at 0.1% strain.
- Amplitude-sweep: strain gradually increased from 0.01% to 100% at 1 rad/s.

Oscillation strain curve data were interpolated using the trace interpolation tool in Origin Pro (version 2022b, OriginLab Corporation, US). Thixotropic properties were measured at an angular frequency of 1 rad/s and a sampling rate of 1 point/s. An initial strain of 0.1% was applied for 5 min, after which the hydrogel was exposed to 11 oscillation cycles alternating between 100% (1 min) and 0.1% strain (10 min). The total test duration was 3,600 s per sample. Stability studies consisted of monitoring the samples relative to their initial state.

2.7. Phase-contrast microscopy

Polyp hydrogel biomaterials were analyzed using a Leica DMI3000 B inverted microscope equipped with a 6-position M25 objective turret (Leica Camera AG, Germany). Illumination was provided by a 12 V/100 W halogen lamp with a manual field diaphragm. The microscope was operated in phase-contrast mode. Images were processed and analyzed using ImageJ software (version 1.54p; imagej.net) to evaluate the micropropagated tissue.

2.8. Epifluorescence microscopy

Biomaterials were examined using the EVOS epifluorescence microscope (EVOS epifluorescence

microscope, Thermo Fisher Scientific, US). Images were captured using a 5-position automated objective turret with a focus mechanism capable of sub-micron resolution (0.150 μm). Epifluorescence microscopy was performed using the following excitation/emission filter sets: Green fluorescence (Ex: 470 nm, Em 525 nm) and chlorophyll (Ex: 585 nm, Em 624 nm). Phase-contrast mode was also employed. All filters were sourced from Thermo Fisher Scientific (US). Image analysis of the micropropagated tissue was performed using ImageJ software.

2.9. Spectrophotometry

Polyp biomaterials were analyzed using a PHERAstar FS microplate reader (PHERAstar FS Microplate Reader, BMG Labtech, Germany). The fluorescence intensity of each well was measured through bottom scanning using specific optical modules. Native polyp green fluorescence was assessed at 485 nm excitation and 520 nm emission, while symbiotic chlorophyll fluorescence was measured at 570 nm excitation and 680 nm emission. These wavelengths were selected based on previously reported values for the coral fluorescence.[24] The optimal focal height was determined automatically, and total fluorescence intensity was measured with 10 flashes per scan point. Data were analyzed using the MARS Data Analysis Software (MARS Data Analysis Software, BMG Labtech, Germany).

2.10. MINI-PAM II photosynthesis yield analyzer

The health of zooxanthellae (the symbiotic microalgae within corals) was examined using a MINI-PAM II instrument (Heinz Walz GmbH, Germany). The instrument utilizes a red light-emitting diode (655 nm) to measure photosynthetic yield. Variable chlorophyll fluorescence of photosystem II (PSII) was assessed using pulse amplitude modulation (PAM) fluorometry (Mini-PAM-II, Heinz Walz GmbH, Germany). To ensure that PSII was in an open state, samples were dark-adapted for 10 min following exposure to aquarium lights. The maximum photochemical efficiency (Fv/Fm) was then calculated using Equation I, where Fm and F_0 represent the maximal and minimal PSII fluorescence of dark-acclimated microencapsulated zooxanthellae, respectively. This method was adapted from previously reported procedures for PAM measurements.[25,26]

$$\left(\frac{F_v}{F_m}\right)=\left(\frac{F_m-F_0}{F_m}\right) \quad \text{(I)}$$

2.11. 3D bioprinting

Bioprinting experiments were conducted using a robotic 3D bioprinter (Dobot, China). The bioprinter comprised a five-degrees-of-freedom robotic arm, a custom-designed dual-coaxial nozzle, microfluidic pumps, and a stirring hot plate (IKA® RCT basic, XXX, IKA-Werke GmbH & Co. KG, Germany). The robotic arm was controlled via Repetier-Host, while printing files were designed in SolidWorks and converted to g-code using the Slic3r and Repetier software (version 1.4.18, Hot-World GmbH & Co. KG, Germany). The dual-coaxial nozzle was fabricated following a previously reported design,[11] with slight modifications for polyp-laden bioprinting. It consisted of two outlets and one inlet. The first nozzle comprised an 18G nozzle outlet (1,270 μm outer, 965 μm inner diameter) for the peptide solution and a 21G nozzle inlet (820 μm outer, 510 μm inner diameter) for the PBS solution. The 21G nozzle was connected to the 18G nozzle, where ionic-driven hydrogel crosslinking occurred. Together, they formed the first part of the dual-coaxial nozzle. The second part consisted of a single 18G nozzle (1,270 μm outer, 965 μm inner diameter).

After the bail-out, *S. pistillata* coral polyps formed spheroids between 200 and 600 μm in diameter, and the reported nozzle dimensions were found to be suitable for extrusion without compromising polyp viability (Figure S1). The nozzle configuration enabled smooth extrusion of bail-out polyps while minimizing clogging risks associated with polyp size. Polyps were successfully extruded without evidence of bursting or clogging.

Commercial microfluidic pumps were operated in automated pulse mode using a square-wave function.[27] The dual-coaxial nozzle was connected to the pumps through three 1,000 μm-diameter microfluidic tubes (Figure S1). Based on the reported viscosity[11] and polyp dimensions, optimized pumping flow rates were determined: 40–45 μL/min (peptide solution), 15–20 μL/min (5× PBS), and 30 μL/min (FSW with polyps). All 3D bioprinting experiments were performed at 27°C. Notably, the interaction between PBS and the peptide solution inside the nozzle resulted in hydrogel formation required for extrusion-based bioprinting.[11] Efficient extrusion of individual polyp units depended on maintaining the optimized flow rates established in the present study.

For cell extraction, a 1 ml syringe filled with FSW was used to gently flush cells through the tubing. Coral skeletons were treated with bleach overnight, washed three times with water, immersed in ethanol for 1 h, and washed again three times with FSW. The coral skeletons were then left in water overnight and subsequently stored at room temperature. Tweezers were sterilized using a Panasonic MLS-3781L autoclave (Japan) at 121°C for 15 min.

2.12. Statistical analysis

Statistical analyses and data visualization were performed using OriginPro 2022b software (OriginLab Corporation, US). Multiple comparisons of population means were

conducted using Tukey's test, with statistical significance set at $p<0.05$.

3. Results and discussion

3.1. Polyp microencapsulation and 3D bioprinting

An overview of the developed strategy and the coral anatomy is shown in Figure 1. The polyp bioink microencapsulation and 3D bioprinting strategy, based on ultrashort peptide-derived bioinks for coral regeneration and polyp culture, is shown in Figure 1A. These bioinks have been extensively used in cell culture and tissue engineering with human cells.[11,28] The primary advantages of formulating bioinks with synthetic peptide-based hydrogels include their bioinertness, biocompatibility, ability to self-assemble into 3D structures, low immunogenicity, minimal batch-to-batch variation compared to naturally derived bioinks, and inherent tendency to accelerate fiber formation in the presence of PBS.[29] In particular, ultrashort self-assembling peptides, recognized for their low immunogenicity, have been widely applied in medicine and, more recently, in environmental technologies such as underwater adhesives.[11,30] Therefore, employing self-assembling peptides composed of natural amino acids offers an interesting strategy for underwater environmental applications. Although recent research has highlighted the successful development of calcium carbonate-based coral-like skeletons and the 3D bioprinting of symbiont-laden bionic coral hydrogels,[13,19,31,32] there are, to date, no reports describing the development of a polyp–symbiont-laden 3D bioprinted biomimetic interphase. Here, we underline the emerging role of ultrashort peptide-based bioinks, in combination with biofunctionalized bioinks, for developing coral-like microenvironments that could serve as a groundwork for future coral tissue transplantation technologies.

A schematic representation of coral polyp anatomy (Figure 1B) and images of a native *S. pistillata* coral polyp (Figure 1C and D) are provided to illustrate the biological context. In these images, green fluorescence highlights the polyp tissue (Figure 1C), while red fluorescence identifies the symbiotic microalgae (Figure 1D).

We evaluated multiple peptide bioink scaffolds for structurally stability under seawater conditions. Bail-out polyps were then microencapsulated in hydrogel-based bioinks to develop polyp-inspired biomaterials. Comparative experiments were performed using two polyp species (*S. pistillata* and *P. verrucosa*), with both individual polyps and clustered configurations tested to enhance survival. The resulting biomaterials were monitored *in vitro* for 45 days, with morphology and

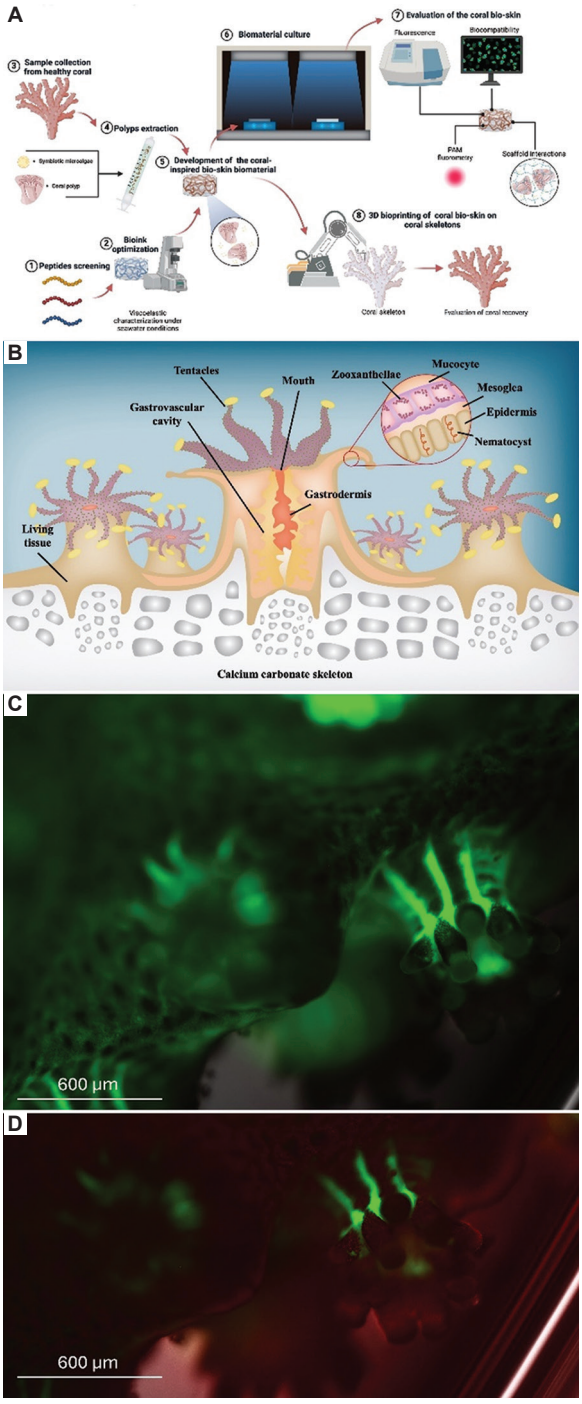

Figure 1. Development of a coral-inspired bio-skin biomaterial to support coral regeneration. (A) Schematic overview of the strategy for developing a coral bio-skin biomaterial to support coral tissue regeneration. (B) A designed illustration of the polyps. (C) Native *Stylophora pistillata* coral polyps, identified by their green autofluorescence, and (D) their symbiotic zooxanthellae, exhibiting a characteristic red fluorescence, are shown on top of their calcium carbonate skeleton. Scale bars: 600 µm; magnification: 10×. The Biorender software was used to prepare Figure 1A.
Abbreviation: PAM: Pulse amplitude modulation.

fluorescence (native green tissue and zooxanthellae) assessed.

Our results identified at least eight peptide-based bioinks as biocompatible with polyps. The best-performing bioinks were selected based on both biocompatibility and mechanical stability (viscoelasticity and degradation resistance) under seawater conditions, making them suitable for 3D bioprinting applications. Furthermore, we optimized a robotic-assisted 3D printer for polyp bioprinting, detailing the optimization process. The most effective combination of bioink and polyp species (Table 2) was then employed to 3D bioprint a unique coral bio-skin on top of coral skeletons, providing a potential strategy to support coral regeneration.

3.2. Bioinks' stability under seawater conditions

Thirteen peptide compounds were selected to create hydrogel-based scaffolds for polyp microencapsulation,

Table 2. Top-performing bioinks for polyp cultivation

Coral polyp specie	Top-performing bioinks	Bioink properties under seawater conditions	Polyp micropropagation	Polyp morphology	Polyp survival time
Stylophora pistillata	B2	Stiffer scaffold (10 kPa), biocompatible, pH 7.7	3.81 mm^2 with visible zooxanthellae spreading through the micropropagated surrounding tissue	Polyp conserves its morphology with signs of emitted green fluorescent protein (GFP) from its tentacles and high zooxanthellae density	Up to 24 days
	B5	Soft scaffold (1 kPa), biocompatible, pH 7.7	2.4 mm^2, visible zooxanthellae spreads through the micropropagated surrounding tissue	Polyp conserves its morphology with signs of emitted GFP from its tentacles and high zooxanthellae density	
	B8	Soft scaffold (1 kPa), collagen-mimetic, biocompatible, pH 7.9	4.16 mm^2, visible zooxanthellae spreads through the micropropagated surrounding tissue	Polyp conserves its morphology with signs of emitted GFP from its tentacles and high zooxanthellae density, signs of potential skeletongenesis underneath	
	B9	Soft scaffold (1 kPa), fibronectin-derived RGDS epitope promoting cell adhesion, biocompatible, pH 7.8	3.53 mm^2, visible zooxanthellae spreads through the micropropagated surrounding tissue	Polyp conserves its morphology with signs of emitted GFP from its tentacles and high zooxanthellae density, signs of potential skeletogenesis underneath	
Pocillopora verrucosa	B2	Stiff scaffold (10 kPa), biocompatible, pH 7.7	4.23 mm^2, visible zooxanthellae spreads through the micropropagated surrounding tissue	Polyp conserves its morphology, contracted tentacles, and high zooxanthellae density	Up to 12 days
	B3	Soft scaffold (1 kPa), biocompatible, pH 7.7	2.41 mm^2, visible zooxanthellae spreads through the micropropagated surrounding tissue	Polyp conserves its morphology, contracted tentacles exhibit GFP, and high zooxanthellae density	
	B4	Soft scaffold (1 kPa), biocompatible, low adhesion, pH 7.7	2.12 mm^2, visible zooxanthellae spreads through the micropropagated surrounding tissue	Polyp conserves its morphology, contracted tentacles, and high zooxanthellae density	
	B6	Soft scaffold (1 kPa), biocompatible, pH 7.6	3.17 mm^2, visible zooxanthellae spreads through the micropropagated surrounding tissue	Polyp conserves its morphology, contracted tentacles, and high zooxanthellae density	
	B8	Soft scaffold (1 kPa), collagen-mimetic, pH 7.9	3.77 mm^2, visible zooxanthellae spreads through the micropropagated surrounding tissue	Polyp conserves its morphology, contracted tentacles exhibit GFP, and high zooxanthellae density	
	B11	Soft scaffold (1 kPa); laminin-derived YIGSR epitope promoting cell adhesion, migration, and differentiation; biocompatible, pH 7.9	4.59 mm^2, visible zooxanthellae spreads through the micropropagated surrounding tissue	Polyp conserves its morphology, contracted tentacles, and high zooxanthellae density	

resulting in the development of bioinks with unique properties for 3D polyp culture (Table 1). Bioinks B1–B8 and B13 were composed of self-assembling peptides 1–8 and 13, respectively, while bioinks B9–B12 were prepared by mixing peptides 9–12 with peptide 1 or 3. Peptides 9–12 were synthesized by attaching biofunctional motifs to the ultrashort peptide compounds 1 and 3. On their own, peptides 9–12 lacked self-assembling capacity; however, when mixed with ultrashort peptides 1 or 3 at defined ratios, they formed bioinks B9–B12.

The bioactive motifs incorporated included RGDS (a fibronectin-derived epitope that mediates cell adhesion and binding), FOGER (a collagen-derived epitope), and YIGSR (a laminin-derived epitope that promotes cell adhesion, migration, and differentiation). Under seawater conditions, bioinks B1–B12 successfully formed hydrogels, whereas bioink B13 did not (Figure 2). Bioinks B1–B3 exhibited the highest stability, retaining their structural integrity without visible degradation or dissolution for over 30 days in seawater (Tables 1 and S1). In contrast, bioinks B4 and B6 formed hydrogels that dissolved in less than 14 days and 24 h, respectively.

The nine rationally designed tetrameric peptides studied (B1–B9, B13) are amphiphilic, comprising hydrophobic and hydrophilic domains.[11] Depending on their sequence, the C-terminus carried either a positively charged residue (B1–B9) or a negatively charged residue (B13). While charged amino acids and pH strongly influence peptide aggregation and assembly,[33] these tetramers assembled exclusively through amphiphilic-driven antiparallel stacking stabilized by van der Waals and hydrogen bonding interactions, consistent with Hauser *et al.*[9] Although previously studied under physiological conditions (pH 7.4) for human cell culture,[11] here they also demonstrated stable assembly under seawater conditions (Tables 1 and S1), to our knowledge for the first time. When FSW was combined with a small amount of PBS (1:10 ratio), the pH ranged between 7.65 and 7.9, depending on the bioink used (Figure S2). This range lies between physiological pH (7.35 to 7.45) and natural seawater (7.78 to 8.21).[34,35] However, even small pH shifts (0.5–1 units) have been reported to negatively affect marine species productivity and community composition.[36] It is important to note that PBS was added only to accelerate bioink formation for subsequent 3D bioprinting; seawater

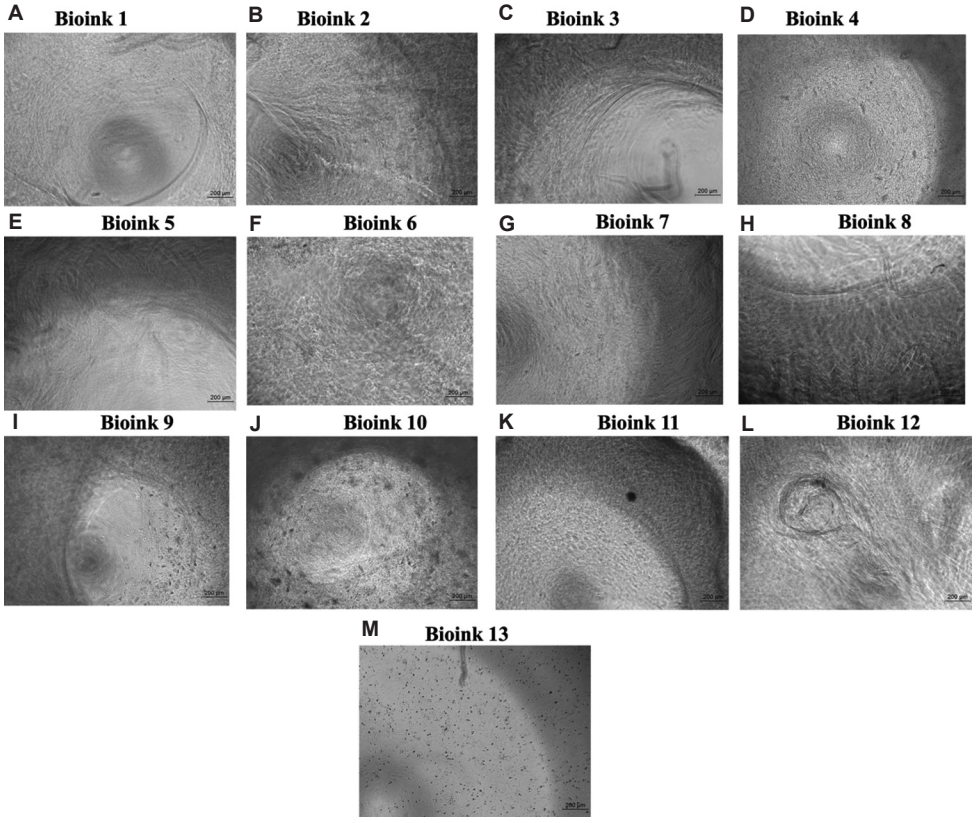

Figure 2. Bioinks under seawater conditions. Bioinks B1–B12 (A–L) contain hydrophilic amino acid (lysine) as the C-terminal residue, whereas bioink B13 (M) contains hydrophilic amino acid (glutamic acid) at the C-terminus. Scale bars: 200 μm; magnification: 20×.

alone can also induce self-assembly due to its natural salt content and the peptides' intrinsic properties. However, using seawater alone may reduce control over the gelation process and slightly alter pH, which could be a limitation for translation applications.

The remarkable stability of these bioinks arises primarily from the rational design of ultrashort self-assembling peptides, which contain a hydrophobic N-terminal tail and a polar C-terminal residue.[11,28,37,38] Even a single amino acid substitution can significantly alter molecular self-assembly and viscoelastic properties.[39] The presence of certain amino acids significantly enhances bioink stability and stiffness under seawater conditions at 27°C. In particular, the exceptional stability of bioink B2 is attributed to the cyclohexylalanine (Z) residue. Bioink B2 outperformed almost identical sequences differing by only one amino acid, as well as bioink B3, which differs from B2 at two positions. Although bioinks B2, B3, and related bioinks remained structurally stable under seawater conditions, they exhibited distinct viscoelastic properties, particularly in storage modulus. Structurally, the Z residue in B2 features a cyclohexane ring, in contrast to the aromatic benzene ring of phenylalanine in B3.[40] These results suggest that ultrashort peptides containing two adjacent cyclohexylalanine residues readily form robust bioinks suitable for potential seawater applications.

Cyclohexylalanine, a synthetic amino acid not naturally present in the human proteome, has demonstrated remarkable biocompatibility with various human cells and may also be compatible with other biological systems, such as coral polyps.[11] Therefore, bioinks incorporating these residues offer distinct advantages for underwater applications. By contrast, bioink B13, which contains an amphiphilic peptide with glutamic acid (a negatively charged residue) at the C-terminus, fails to assemble under seawater conditions (Table S1). In comparison, peptides with a positively charged lysine residue at the C-terminus successfully formed hydrogel-based bioinks under seawater conditions. Depending on the peptide sequence, some of these lysine-containing bioinks remained structurally stable without visible deformation for more than 30 days, while others dissolved within 2 weeks or even less than 24 h (Tables 1 and S1). Overall, most bioinks retained at least 75% of their structure for 30 days in seawater. This stability highlights their potential for field applications, where they could provide localized, durable scaffolds for targeted coral restoration. Accordingly, amphiphilic peptide sequences with positive C-terminal charges are considered promising candidates for seawater bioprinting applications.

3.3. Polyp microencapsulation and 3D bioprinting after bail-out

Polyps were encapsulated using two different strategies: as clustered entities and as individual units. Previous studies have reported the use of epifluorescence microscopy and spectrophotometry to monitor the health status of bail-out polyps.[6,7] Therefore, two complementary methods were employed in this study to assess polyp health after bail-out and subsequent microencapsulation. These methods included (i) quantitative monitoring of the polyp's natural green fluorescence and the chlorophyll red fluorescence of the symbiotic zooxanthellae, and (ii) qualitative assessment using phase-contrast and epifluorescence microscopies to evaluate polyp morphology (Figure 3). As controls, fluorescence was monitored in FSW (Figure 3A), cultured polyps suspended in seawater (Figure 3B), native coal fragments (Figure 3C), and scaffolds without polyps.

Natural *S. pistillata* coral fragment before (Figure 4A) and after polyp bail-out (Figure 4B) were imaged, along with their structural details (Figure 4C and D). After the bail-out, suspended polyps adopt a spherical shape and detach from the natural coral skeleton. Bail-out polyps from both *S. pistillata* and *P. verrucosa* were observed spinning continuously in seawater without re-settling (Figure 4E and F).

In contrast, microencapsulated polyps were immediately provided with a substrate for anchorage and reoriented their oral region toward the incident light source (Figure 5). By comparison, *S. pistillata* and *P. verrucosa* polyps cultured in FSW underwent cellular lysis and membrane rupture within 5 days (Figures S3 and S4). This degeneration was accompanied by a loss of green fluorescence and a marked increase in red fluorescence (Figure S5). Previous studies have highlighted that the success rate of polyp re-settlement after bail-out is typically low.[3,4] However, when microencapsulated within bioinks, polyps re-settled within 24 h. This enhanced re-settlement is attributed to their direct contact with bioink fibers, which serve as a suitable substrate for instantaneous polyp re-settlement (Figure 5). Comparable behavior has been observed in *Pocillopora damicornis* polyps cultured in a coral-on-a-chip microfluidic device, where microscopy was used to track native green fluorescent protein and chlorophyll autofluorescence (red) over 6 weeks.[6] The red fluorescence of bail-out polyps has been linked to algae chlorophyll, as seen in symbiotic zooxanthellae.[6,7]

3.4. Polyp biomaterial cultivation

Unlike other methods, such as suspending polyps in water, the use of self-assembling peptide-based bioinks for bail-

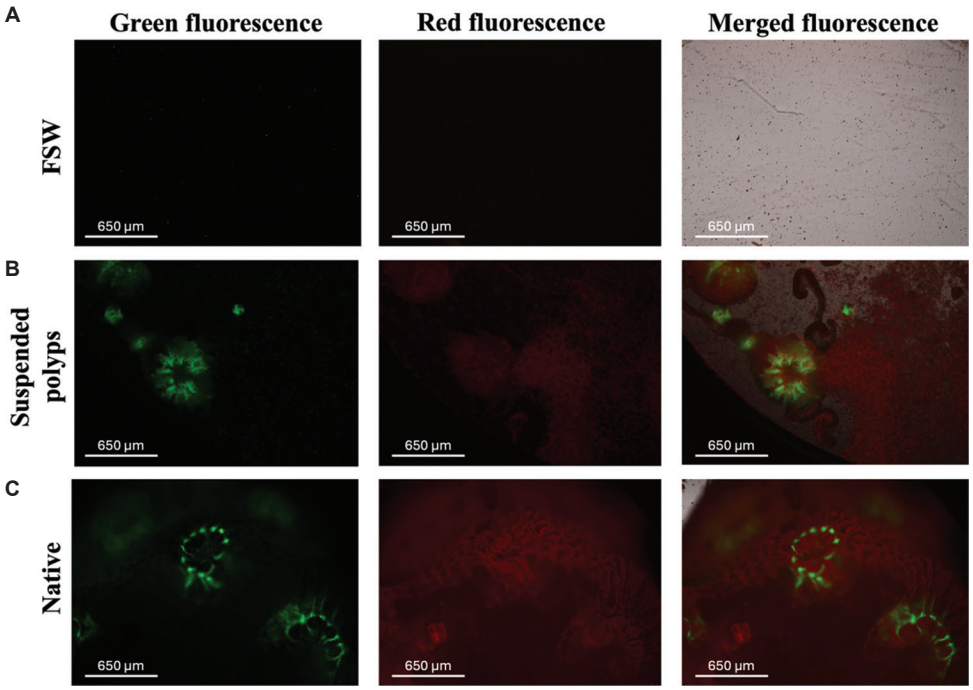

Figure 3. Experimental controls. (A) Filtered seawater (FSW); (B) suspended *Stylophora pistillata* polyps after polyp bail-out; and (C) native *S. pistillata* coral fragment. Scale bars: 650 µm; magnification: 10×.

out polyps promotes instantaneous interaction with the scaffold surface. This facilitates rapid reattachment and subsequent micropropagation. *S. pistillata* polyps cultured in FSW (Figure 5A) were compared to microencapsulated *S. pistillata* polyps (Figure 5B). The microencapsulated polyps maintained their morphology and displayed native green fluorescence (Figure 5C) for up to 24 days. In contrast, *P. verrucosa* polyps cultured in FSW (Figure 5D) were compared with their microencapsulated counterparts (Figure 5E). Suspended polyps exhibited lysis when cultured in FSW (Figures S3 and S4), whereas microencapsulated polyps preserved their spherical morphology and displayed characteristic native green fluorescence in their tentacles (Figure 5E and F).

Structurally, *S. pistillata* polyps retained their shape when cultured in bioinks (Figure 6). When microencapsulated (Figure 6A and B), tissue production was accelerated when at least two polyps were cultured in close proximity (Figure 6C and D). These findings demonstrate that microencapsulated *S. pistillata* polyps maintained their morphology and self-generated fluorescence for up to 24 days. The most effective bioinks for polyp cultivation were bioinks B2, B5, B8, and B9. These bioinks promoted the formation of surrounding tissue within *S. pistillata* polyps within 6 days (Figure 6E-H), indicating active polyp micropropagation. Bioinks B2, B5, and B8 were composed of ultrashort self-assembling peptides without additional biofunctionalities, whereas bioink B9 incorporated the fibronectin-derived RGDS adhesion motif covalently attached to the scaffold. Our results suggest that *S. pistillata* polyps adapted to both stiff and soft bioink scaffolds, though stiff bioinks provided a microenvironment more closely resembling the interface between the coral tissue coenosarc and the natural calcium carbonate skeleton. The biofunctional RGDS motif, known to mimic integrin recognition sites, plays a key role in mediating cell adhesion. Although this motif has primarily been studied in mammalian cells, our results indicate that RGDS also enhances polyp re-settlement. This finding highlights the potential of incorporating biofunctionalized motifs into biomimetic scaffolds to enhance bail-out polyp micropropagation. For instance, the integrin β subunit, which has been identified in several coral species, is involved not only in cell adhesion, fertilization, and symbiont uptake but also in cell–extracellular matrix interactions.[41-44] Therefore, combining RGDS with either soft or stiff scaffolds could significantly enhance integrin-mediated recognition of biomimetic scaffolds by bail-out polyps and accelerate tissue micropropagation. Further experiments aiming to recreate the coenosarc microenvironment of *S. pistillata* should consider stiff bioinks supplemented with RGDS motifs. The initial total area of an *S. pistillata* bail-out polyp was 0.11 mm^2, which increased significantly after 24 days of cultivation due to micropropagation (Table 2).

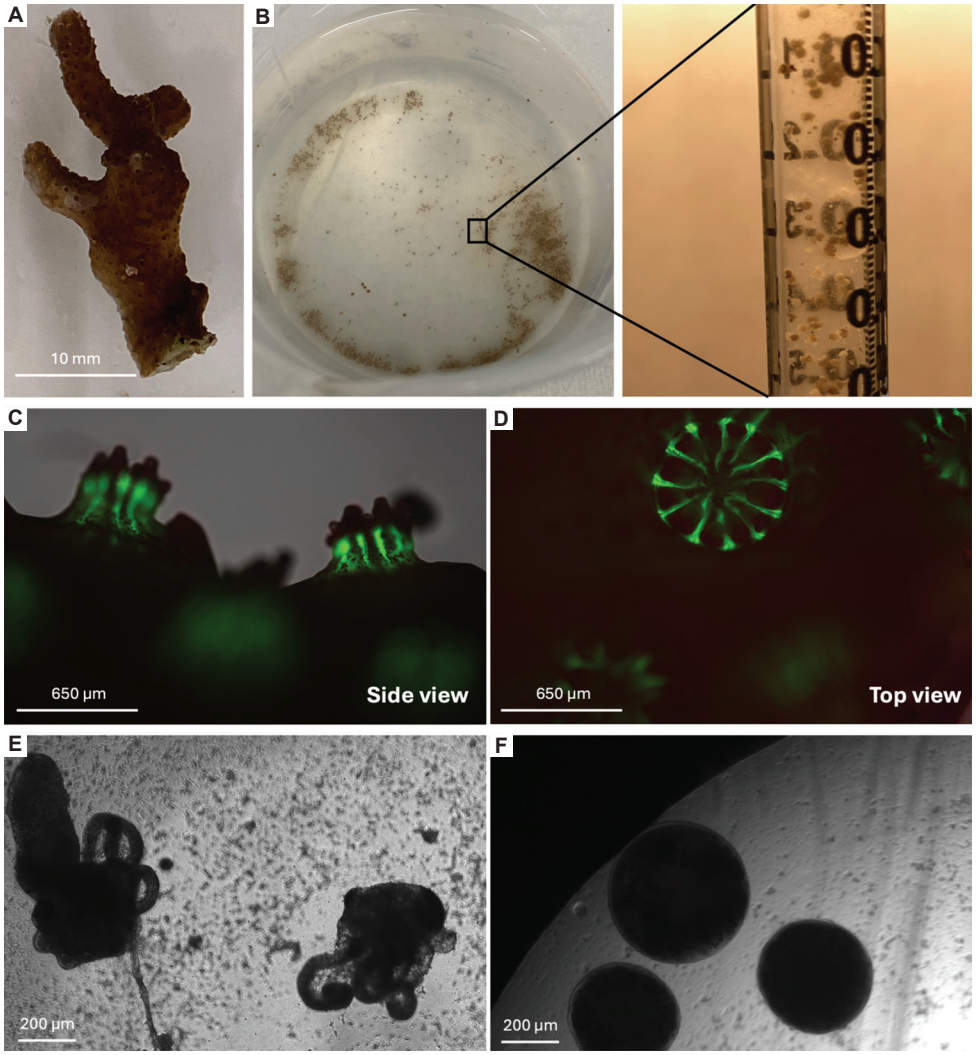

Figure 4. Extracted polyps. (A) Native *Stylophora pistillata* coral fragment. (B) Extracted polyps batch. *S. pistillata* polyps on the calcium carbonate skeleton: Side view (C) and top view (D). *S. pistillata* (E) and *Pocillopora verrucosa* polyps (F). Scale bars: (C & D) 650 µm, (E & F) 200 µm; magnification: 10× (C & D), 20× (E & F).

The top-performing bioinks for *P. verrucosa* polyps were B2, B3, B4, B6, B8, and B11 (Figure 7). Polyps were microencapsulated (Figure 7A), and after 3 days of culture, micropropagated tissue was observed (Figure 7B). Tissue production accelerated when at least two polyps were cultured in close proximity (Figure 7C), although the extent varied depending on the underlying peptide sequence of each bioink (Figure 7D-I). Based on these findings, microencapsulated *P. verrucosa* polyps maintained their morphology and displayed self-generated fluorescence for up to 12 days. Bioinks B2, B3, B4, B6, and B8 consisted of ultrashort self-assembling peptides without additional biofunctional motifs, whereas B11 incorporated the laminin-derived YIGSR cell adhesion motif. *P. verrucosa* polyps responded favorably to both stiff and soft scaffolds. It aligns with reports that the natural coral skeleton microstructure of this coral contains radially arranged calices with a gradient of compressive properties.[45] As a result, the coral exhibits both high strength and localized deformation due to its natural calcium carbonate architecture. This is congruent with our results that bail-out polyps from this coral species exhibited affinity for both soft and stiff bioinks.

The YIGSR motif, previously applied in mammalian organoid culture, also promoted polyp re-settlement in *P. verrucosa*.[46] Our findings indicate that the use of a moderately stiff bioink in combination with the YIGSR motif facilitated attachment, successful re-settlement, and subsequent micropropagation. Further studies aiming to create a biomimetic microenvironment that closely resembles the coenosarc tissue of *P. verrucosa* should

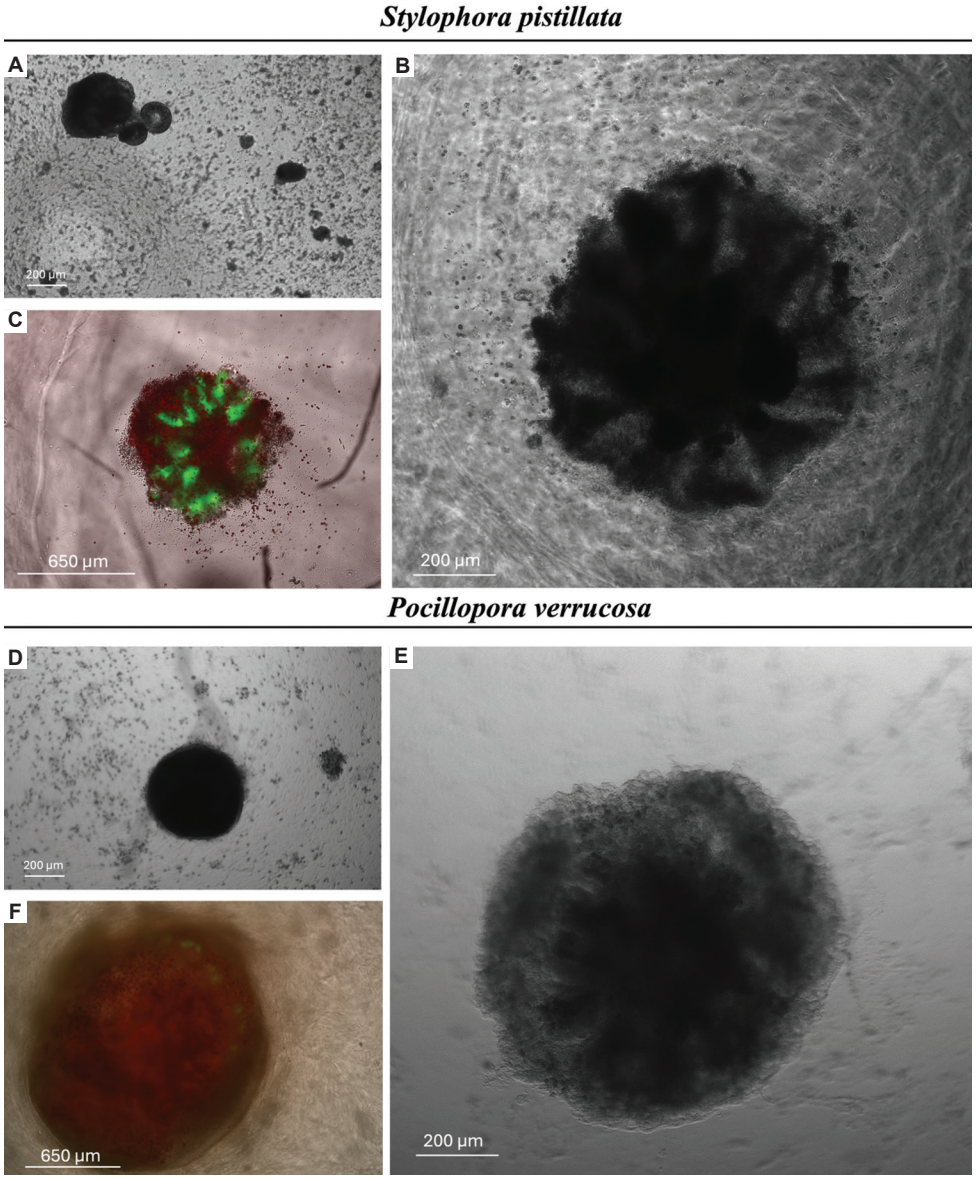

Figure 5. Microencapsulated *Stylophora pistillata* and *Pocillopora verrucosa* polyps. (A) Suspended *S. pistillata* polyp in seawater. Scale bars: 200 µm; magnification: 20×. (B) Phase-contrast imaging of a microencapsulated *S. pistillata* polyp in bioink B2 after 24 h. Scale bars: 200 µm; magnification: 20×. (C) Epifluorescence imaging of microencapsulated coral tissue (green) and zooxanthellae (red). Scale bars: 650 µm; magnification: 10×. (D) Suspended *P. verrucosa* polyp in seawater. Scale bars: 200 µm; magnification: 20×. (E) Phase-contrast imaging of a microencapsulated *P. verrucosa* polyp in bioink B3 after 24 h. Scale bars: 650 µm; magnification: 10×. (F) Epifluorescence imaging of the microencapsulated coral tissue (green) and zooxanthellae (red). Scale bars: 200 µm; magnification: 20×.

consider scaffolds with a stiffness gradient combined with YIGSR binding motifs. The initial area of a *P. verrucosa* bail-out polyp was 0.18 mm^2, which increased significantly after 12 days of cultivation due to micropropagation (Table 2).

For both polyp species, accelerated micropropagation (Figures 6C and 7C) and inter-polyp interactions (Figures 6D and 7D) were observed when bail-out polyps were cultivated within 0.5 mm of each other inside bioink scaffolds. Conversely, polyps cultured in FSW underwent lysis within 24 h (Figures S3-S5). These findings highlight the potential of biofunctionalized bioinks for supporting polyp cultivation.

Fluorescence data supported these findings (Figure 8). In *S. pistillata*, green fluorescence decreased gradually, reaching baseline levels by day 45 (Figure 8A). In contrast, *P. verrucosa* polyps exhibited a steep decrease in green fluorescence after 5 days (Figure 8E). These results indicate

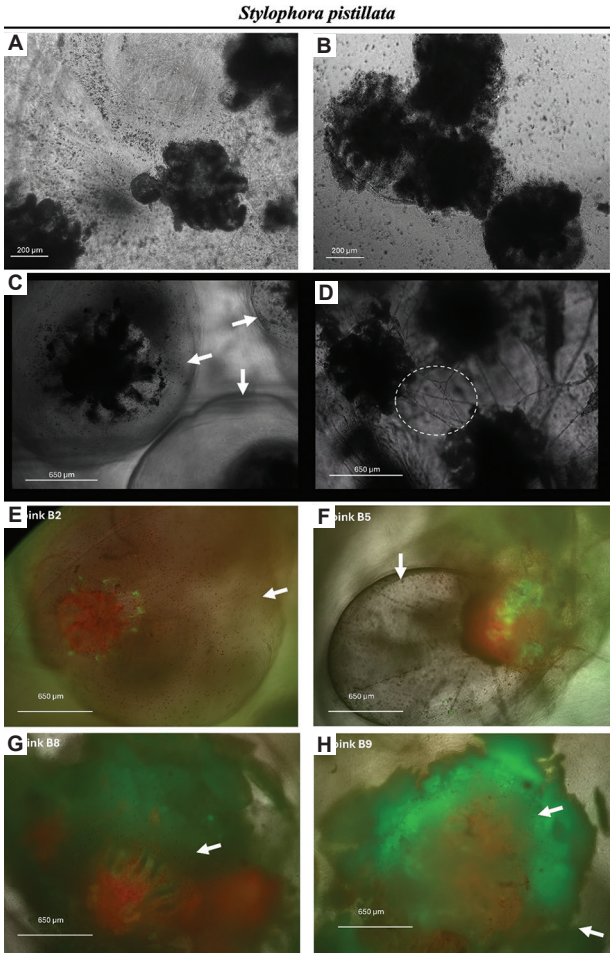

Figure 6. Culture of *Stylophora pistillata* polyps in cluster form. (A) Day 0; (B) after 24 h; (C) surrounding halo formation on day 6; (D) inter-polyp interactions after 6 days. *S. pistillata* polyps in the best-performing bioinks after 24 days: (E) B2, (F) B5, (G) B8, (H) B9. White arrows indicate surrounding halo micropropagation (C, E–H), and the dashed circle denotes inter-polyp connections (D). Scale bars: (A & B) 200 µm, (C–H) 650 µm; magnification: 20× (A & B), 10× (C–H).

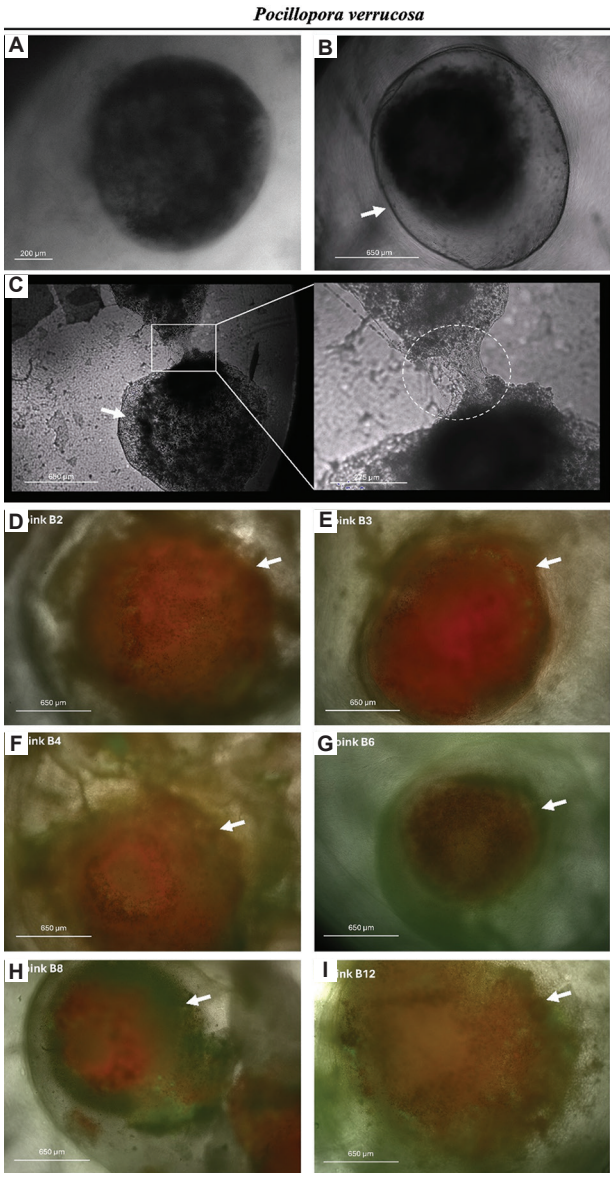

Figure 7. Culture of *Pocillopora verrucosa* polyps in cluster form. (A) Day 0; (B) surrounding halo formation after 6 days; (C) inter-polyp interactions after 6 days; *P. verrucosa* polyps in the best-performing bioinks after 12 days: (D) B2, (E) B3, (F) B4, (G) B6, (H) B8, (I) B11. White arrows indicate surrounding halo micropropagation (B, D-I), and the dashed circle denotes inter-polyp connections (C). Scale bars: (A) 200 µm, (B-I) 650 µm, inset in (C) 275 µm; magnification: (A) 20×, (B-I) 10×, inset in (C) 20×.

that while bioinks can function as biomimetic scaffolds resembling coral coenosarc tissue and sustain bail-out polyps outside of their natural coral skeleton for several days, the current cultivation conditions and scaffold architecture require further refinement to achieve longer-term viability (e.g., polyp cultivation in flow chambers or with integrated calcium carbonate layers).

After encapsulation, both polyp species showed low and unstable red fluorescence, which increased significantly after 5 days. This increase was attributed to chlorophyll autofluorescence from the symbiotic zooxanthellae (Figure 8C and G). Red fluorescence was higher in *P. verrucosa* than in *S. pistillata*. In clustered polyps, red fluorescence decreased after 15 days in *S. pistillata* and after 20 days in *P. verrucosa*, with similar trends observed in single polyps. After this period, red fluorescence increased again, accompanied by a further decrease in green fluorescence.

Of the 13 bioinks tested, eight supported polyp morphology and the formation of surrounding halos. The appearance of surrounding halos, previously documented in bail-out polyps cultured within microfluidic devices,

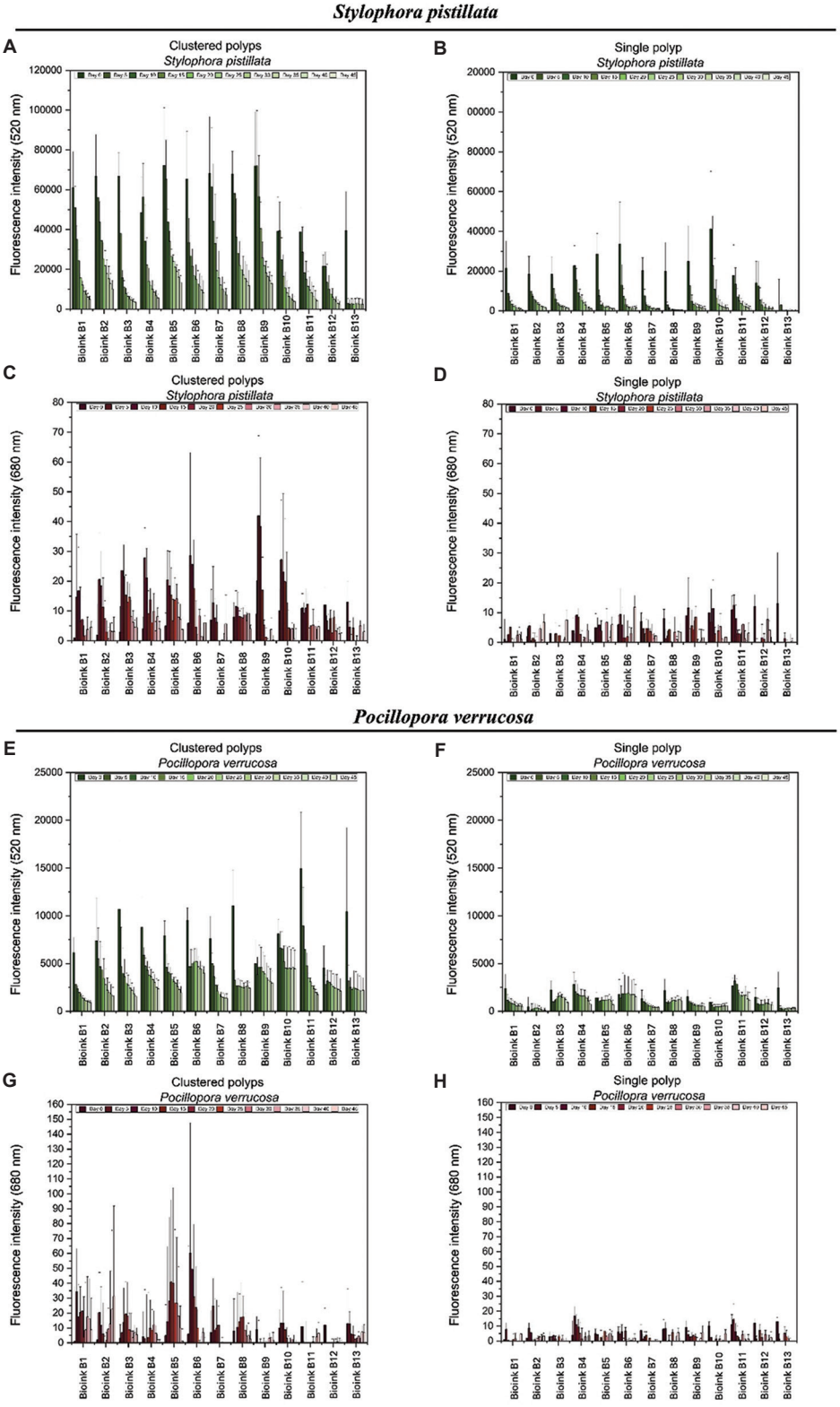

Figure 8. Green and red fluorescence intensity in *Stylophora pistillata* and *Pocillopora verrucosa* polyps. (A–D) S. pistillata polyps cultured in clusters (A, C) and as single units (B, D). (E–H) P. verrucosa polyps cultured in clusters (E, G) and as single units (F, H). Each experiment was performed with replicates of $n = 6$.

is considered an indicator of successful re-settlement and subsequent micropropagation.[6] This occurs because bioinks differ in softness or stiffness and generate fibers of varying thickness, which influence cell adhesion, differentiation, cytocompatibility, and nutrient diffusion within the bioink scaffolds. These parameters collectively create distinct microenvironments for cell growth and proliferation.[11,47-49]

It is suggested that following polyp bail-out, some symbiotic microalgae shut down photosynthesis due to the initial high stress of being outside their natural symbiotic environment within the coral dermis. After 5 days of adjustment, some symbionts from their membrane-bound symbiosomes were released during bail-out and remained present during encapsulation. A similar pattern was observed in bail-out polyps cultured in a microfluidic chip, where symbiont chlorophyll increased post-bail-out.[6] A similar trend was also observed in suspended polyps, where red fluorescence increased while green fluorescence decreased (Figure S5). This change may be attributed to microalgal breakdown under nutrient deprivation. Other studies suggest that corals may even feed on their photosynthetic symbionts under starvation conditions.[50,51]

These observations indicate a potential disruption of symbiosis when bail-out polyps are transplanted into bioinks, leading to species-specific fluorescence dynamics. Furthermore, there appears to be an optimal timeframe during which both polyps and zooxanthellae are in ideal conditions for transfer of this biomaterial under semi-batch conditions to continuous systems (e.g., microfluidic devices or aquaria) that provide enhanced nutrient inflow. A summary of the top-performing bioinks and their compatibility with bail-out polyps in terms of micropropagation, morphology, and survival is presented in Table 2.

3.5. Bioinks' viscoelastic properties under seawater conditions

Based on the preceding results, we selected *S. pistillata* polyps for 3D bioprinting experiments to create a coral-inspired bio-skin biomaterial. For potential *in situ* applications, we evaluated the viscoelastic properties (Figure 9) of the best-performing bioinks for *S. pistillata* polyps, selected according to seawater stability (Table 1) and polyp biocompatibility (Table 2).

Initially, we assessed the ability of each bioink to store energy before deformation, measured by storage and loss modulus. Bioink B2 exhibited a significantly higher storage modulus compared to the other bioinks ($p<0.001$) (Figure S6), indicating superior structural stability under seawater conditions. These findings align with earlier results in the present study, where bioinks containing adjacent cyclohexylalanine (Z) residues demonstrated enhanced stability (Tables 1 and S1). Next, we assessed scaffold network strength by measuring responses to increasing angular frequency. All bioinks displayed low frequency dependence, suggesting the formation of well-organized 3D scaffold networks due to their self-assembling capabilities. Among them, B2 exhibited the strongest network integrity. We also evaluated oscillation strain behavior. All bioinks underwent a transition from solid-like to liquid-like states at different oscillation strains. Bioinks B3, B5, and B9 tolerated higher oscillation stress but exhibited lower structural stability under static conditions. Overall, bioinks B1 and B2 demonstrated the greatest mechanical structural stability under seawater conditions, although both were still capable of transitioning into a liquid state under oscillatory forces. Statistical significance was determined using the Tukey test and is reported in Figure S6.

Our results further indicate that polyps transplanted from their natural coral skeleton to hydrogel-based scaffolds – serving as artificial, biomimetic coral skin – do not immediately die. Instead, the polyps adapt to the scaffold, maintain their morphology, and continue to emit green and red fluorescence for several days. This suggests that their survival could be prolonged under improved conditions, such as open systems with continuous nutrient supply, or by supplementing FSW with additional nutrients.

Transferring these biomaterials to open system conditions is feasible because the bioinks exhibit diverse mechanical and viscoelastic properties depending on their peptide sequence, resulting in distinct stability profiles under seawater (Figure 9 and Table S1). Accordingly, *S. pistillata* and *P. verrucosa* polyps can be maintained in microcapsules for at least 10 days and subsequently transferred to continuous culturing systems. During this period, the polyps retain their shape and fluorescence, though eventual disruption of their symbiotic relationship occurs. Further investigation of the viscoelastic properties of these biomaterials is required to optimize their performance under seawater conditions.

3.6. Development of a coral-inspired bio-skin biomaterial

We achieved the first-of-its-kind 3D bioprinting of coral polyps to create a coral-inspired bio-skin biomaterial (Figure 10). The overall strategy is presented in Figure 10A. The robotic-assisted 3D bioprinting system was optimized specifically for polyp-laden bioprinting (Figure 10B and C). Optimization parameters included pumping speed, robotic arm movement, PBS concentration, gelation speed, nozzle tip dimensions, and nozzle tubing dimensions, all

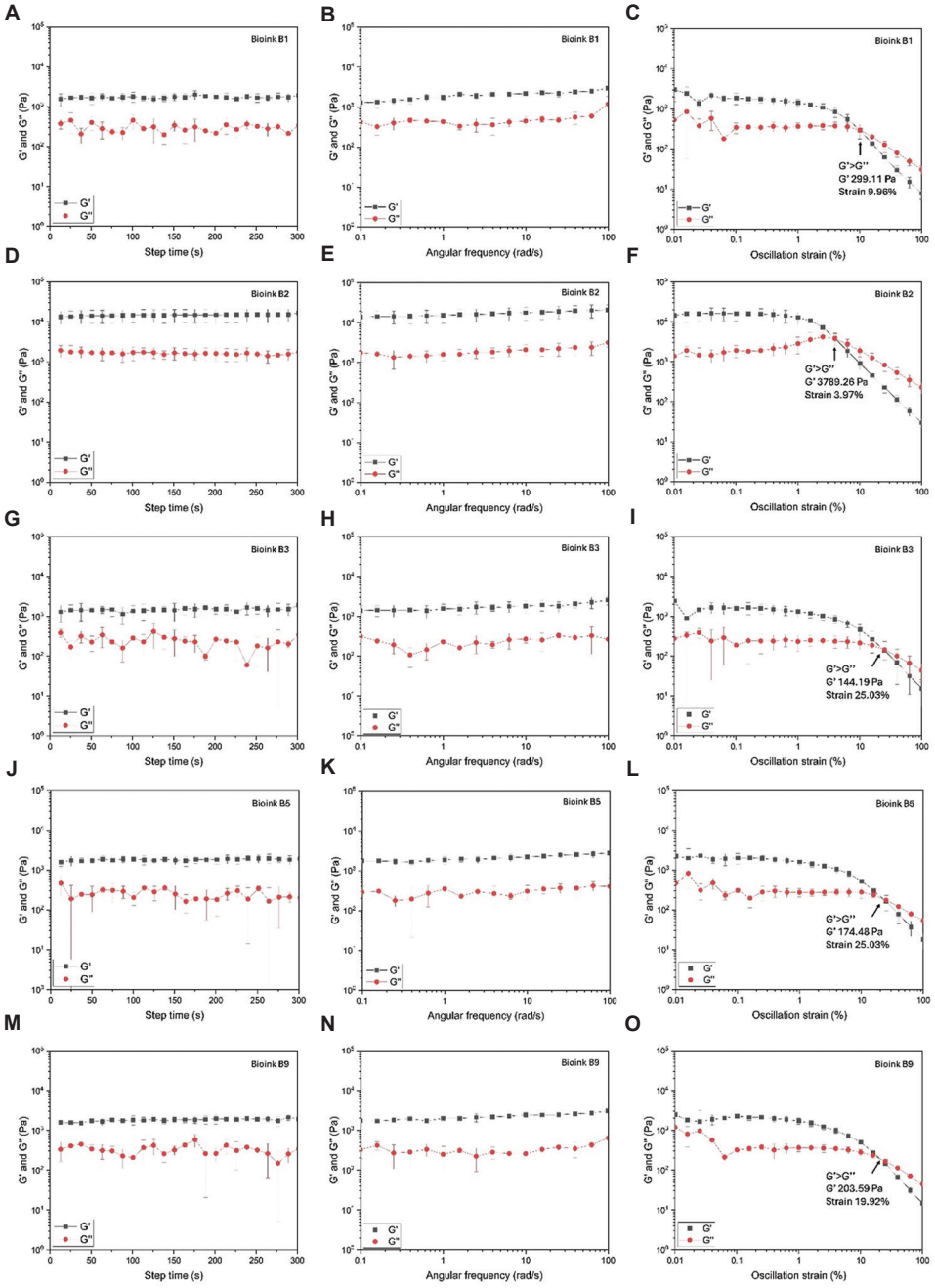

Figure 9. Rheological characterization of top-performing bioinks after 30 days of seawater submersion. Viscoelastic properties were evaluated through step time (A, D, G, J, M), angular frequency (B, E, H, K, N), and oscillation strain (C, F, I, L, O). The turnover points were as follows: B1, 299.11 Pa at 9.96% strain (C); B2, 3789.26 Pa at 3.97% strain; B3, 144.19 Pa at 25.03% strain; B5, 174.48 Pa at 25.03% strain; and B9, 203.59 Pa at 19.92% strain. Experiments were conducted at 27°C with $n = 6$ replicates.

adjusted according to the morphological properties of bail-out *S. pistillata* polyps (Figure S1) and the viscoelastic properties of the selected bioink. In this study, we used the Ac-Ile-Cha-Cha-Lys-NH_2 (IZZK) peptide because of its biocompatibility with polyps, high printability, and stability under seawater conditions. This enabled the successful bioprinting of a polyp-laden coral bio-skin biomaterial directly onto coral skeletons (Figure 10C and D). Under the optimized conditions, the 3D bioprinter was able to deposit polyps without inducing lysis. Although microencapsulated, the polyps retained tentacle movement (Video S1). Thixotropic analysis further revealed that the

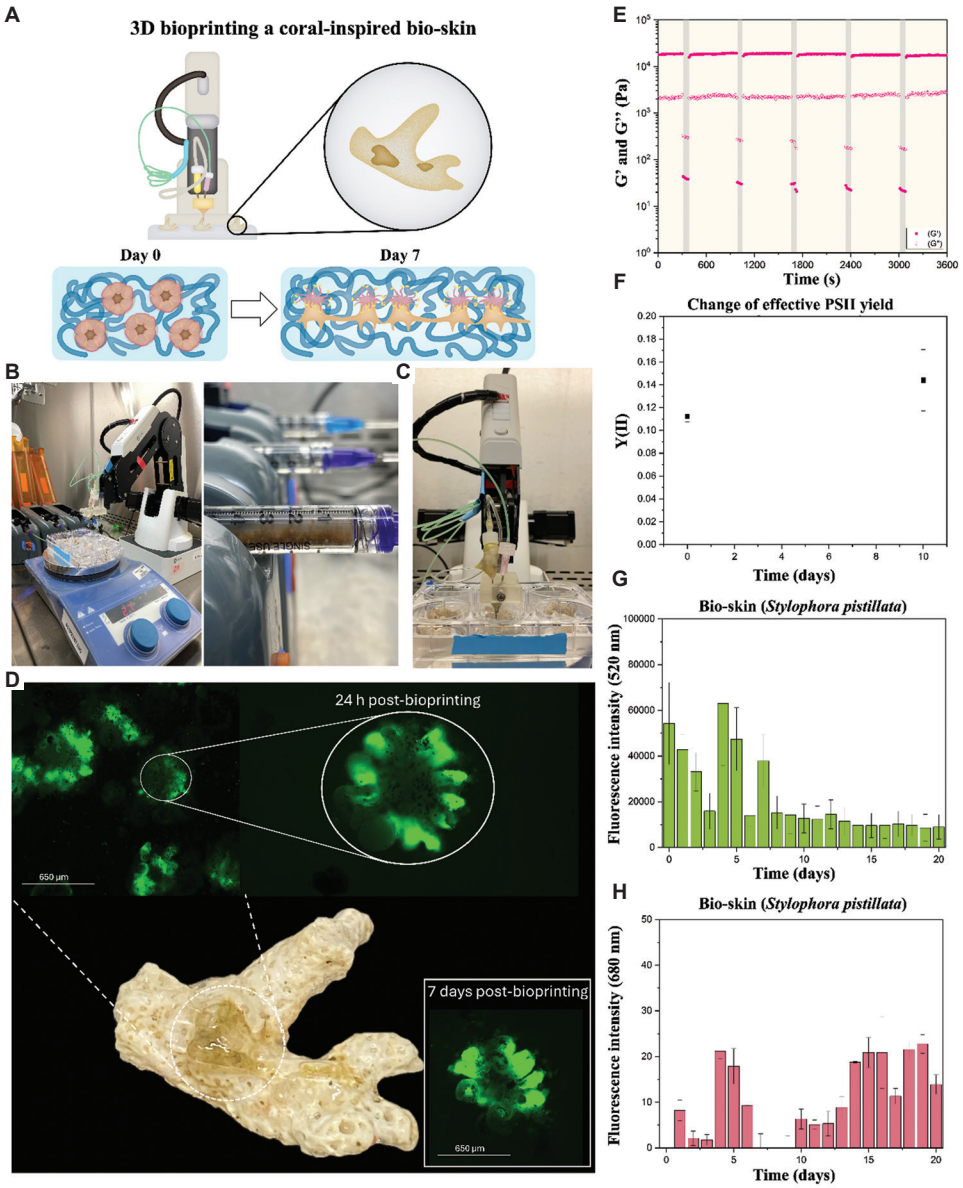

Figure 10. 3D bioprinting of coral-inspired bio-skin on calcium carbonate coral skeletons. (A) A schematical design illustrating the 3D bioprinting of the coral bioskin. (B) 3D bioprinter setup for polyp bioprinting. (D) Bioprinting of coral skin onto coral skeletons. (D) 3D-bioprinted coral-inspired bio-skin containing *Stylophora pistillata* polyps after 24 h and 7 days post-bioprinting. Scale bars: 650 µm, magnification: 10×. (E) Self-healing properties of the polyp bio-skin biomaterial. (F) Effective photosystem II (PSII) yield (Y[II]) of immobilized polyps during a 10-day cultivation period, measured using MINI-PAM-II Photosynthesis Yield Analyzer. (G) Polyp-associated green fluorescence. (H) Zooxanthellae red fluorescence.

combination of polyps and bioink formed a self-healing biomaterial, supporting its potential application *in situ* for regenerating coral substrates (Figure 10E).

In addition, PAM results confirmed that the symbiotic zooxanthellae remained metabolically active and stable after 10 days (Figure 10F). The successful presence of 3D-bioprinted polyps within the coral-inspired bio-skin biomaterial was corroborated by epifluorescence microscopy, further supporting our findings that microencapsulated polyps retain tentacle movement after bioprinting (Video S2). These results were consistent with fluorescence intensity measurements associated with coral tissue and symbionts (Figure 10G and H). Tentacle movement within hydrogel scaffolds can be attributed to the remarkable properties of ultrashort self-assembling peptides, which form nanofibrous 3D scaffolds. These scaffolds not only allow nutrient diffusion through their mesh-like architecture but can also reorganize their

fiber network due to the innate thixotropic nature of the hydrogel scaffolds. However, further research is required to elucidate the effect of bioink thickness on the performance of 3D-bioprinted coral-polyp bio-skins.

Fluorescence analysis revealed a notable decrease in green fluorescence, suggesting that cultivation conditions could be further optimized. Consistent with earlier results, red fluorescence associated with zooxanthellae decreased, likely due to nutrient starvation, and subsequently increased when green fluorescence (Figure 10G) stabilized at low constant levels (Figure 10H).

These findings suggest that the extrusion-based 3D bioprinting process imposes greater stress on polyps compared to manual microencapsulation, reinforcing the need to optimize culture conditions to enhance long-term viability. Nevertheless, this study highlights the potential of 3D bioprinting for generating polyp-laden biomaterials. Under the tested conditions, the 3D-bioprinted biomaterial supported viable polyps for approximately 7 days, sustained solely with FSW as the nutrient source.

Future research should investigate the cultivation of 3D-bioprinted polyp biomaterials under diverse environmental conditions, such as temperature, salinity, and nutrient enrichment, to improve polyp survival after transplantation. Recent progress in this field includes the development of bionic corals fabricated with GelMA-based 3D bioprinting platforms that mimic coral skeletons and incorporate symbionts.[13,14] Other studies have explored calcium carbonate-based materials and bioinks to support coral restoration,[32,52] while antioxidant-enriched biomaterials (e.g., biodegradable composites with curcumin, zein, and polyvinylpyrrolidone) have been formulated to mitigate thermal stress on corals.[22] Advancements in 3D printing and bioprinting technologies have enabled the fabrication of cutting-edge coral-inspired structures and biomaterials for coral restoration. For instance, GelMA-based hydrogels have been employed to replicate living coral tissue and skeletons with micron-scale resolution.[13] Sustainable calcium carbonate-based materials have also been used to print coral-like structures, and bioprinted coral microenvironments have successfully mimicked coral–algal symbiosis.[13,14,19,32,52] Hydrogel-based systems have additionally been engineered to promote the growth of synthetic algal–bacterial consortia.

Coral tissue thickness (covering the coral skeleton) ranges from 100 μm to 0.5 cm, depending on the species. Extrusion-based bioprinting technology can replicate these 3D structures by integrating appropriate biological components with scaffold materials. In this study, we present ultrashort and biofunctionalized peptide-based scaffolds designed specifically for underwater applications, contributing to the development of coral-inspired bio-skin biomaterials. These biomaterials represent a promising platform for coral tissue transplantation and a significant advancement toward *in situ* coral regeneration.

4. Conclusion

We developed a novel method, termed polyp microencapsulation and 3D bioprinting (or abbreviated as PM3D), for bail-out polyp transplantation. Our results revealed that successful polyp micropropagation occurs when multiple polyps are microencapsulated within bioink scaffolds. We identified eight peptide-based bioinks suitable for both polyp micropropagation and 3D bioprinting and analyzed their viscoelastic properties under seawater conditions. Some of the supporting peptide bioinks incorporated bioactive motifs such as RGDS and YIGSR, which are commonly used to mimic the mammalian cellular microenvironment. Interestingly, these bioactive motifs also positively influenced polyp propagation.

The identified peptide bioinks did not harm bail-out polyps and remained stable under seawater conditions. They were able to rapidly form fibers, enabling settlement between bail-out polyps and hydrogel substrates, thus serving as external scaffolds to support polyp growth outside their natural tissue. We also observed changes in red fluorescence following bail-out and subsequent microencapsulation, indicating disruption of the symbiotic relationship between the polyp and zooxanthellae, likely due to nutrient scarcity. Importantly, bioprinted polyps microencapsulated in ultrashort peptide bioinks still exhibited tentacle movement (Videos S1 and S2), depending on scaffold stiffness, thickness, and crosslinker concentration. These parameters can be further optimized to improve polyp viability post-printing. Future research aimed at the long-term cultivation of artificial polyp–bio-skin biomaterials should consider integrating flow-through microfluidic devices to better mimic field-like conditions, incorporating biomimetic coral cues, optimizing biomaterial compositions, and cultivating these biomaterials in nutrient-enriched media.

To advance coral tissue regeneration technologies, we selected the top-performing bioink to 3D bioprint a coral-inspired bio-skin biomaterial onto calcium carbonate coral skeletons. These findings pave the way for coral tissue engineering by harnessing polyp-directed bioinks derived from ultrashort self-assembling and biofunctionalized peptides, which can serve as support scaffolds for future coral tissue transplantation strategies.

Acknowledgments

We thank the Core Labs for providing the high-end research facilities that enabled this work. We would like to thank

Kowther Kahin and Zainab Khan for their contributions to the development of the 3D bioprinting system and dual-coaxial nozzle, as well as to all past and present members of the Bioprinting Team for their contributions to the development of the robotic-assisted 3D bioprinter. We also thank Montserrat del Socorro Valle Perez for the design of some illustrations.

Funding

This research was funded by King Abdullah University of Science and Technology (KAUST) to Charlotte A. E. Hauser. Additional funding was provided by Graz University of Technology (TU Graz) to Christian Baumgartner, and by research start-up funds awarded to Charlotte A. E. Hauser.

Conflict of interest

Charlotte A. E. Hauser is an Editorial Board Member of this journal, but was not in any way involved in the editorial and peer-review process conducted for this paper, directly or indirectly. Separately, other authors declared that they have no known competing financial interests or personal relationships that could have influenced the work reported in this paper.

Author contributions

Conceptualization: Alexander U. Valle-Pérez, Charlotte A.E. Hauser

Formal analysis: Alexander U. Valle-Pérez, Charlotte A. E. Hauser, Manola Moretti, Panayiotis Bilalis

Funding acquisition: Charlotte A. E. Hauser, Christian Baumgartner

Investigation: Alexander U. Valle-Pérez, Sebastian Overmans

Methodology: Alexander U. Valle-Pérez, Panayiotis Bilalis, Sebastian Overmans, Kyle J. Lauersen

Supervision: Charlotte A. E. Hauser

Visualization: Alexander U. Valle-Pérez

Writing–original draft: Alexander U. Valle-Pérez

Writing–review & editing: Alexander U. Valle-Pérez, Charlotte A. E. Hauser, Christian Baumgartner

Ethics approval and consent to participate

Not applicable.

Consent for publication

Not applicable.

Availability of data

Any additional information required to reanalyze the data reported in this paper is available from the corresponding author on reasonable request.

References

1. Mieog JC, Van Oppen MJH, Berkelmans R, Stam WT, Olsen JL. Quantification of algal endosymbionts (*Symbiodinium*) in coral tissue using real-time PCR. *Mol Ecol Resour*. 2009;9(1):74-82.

   doi: 10.1111/j.1755-0998.2008.02222.x

2. Silverstein RN, Correa AMS, Baker AC. Specificity is rarely absolute in coral-algal symbiosis: Implications for coral response to climate change. *Proc R Soc B*. 2012;279(1738):2609-2618.

   doi: 10.1098/rspb.2012.0055

3. Sammarco P. Polyp Bail-Out: An escape response to environmental stress and a new means of reproduction in corals. *Mar Ecol Prog Ser.* 1982;10:57-65.

   doi: 10.3354/meps010057

4. Serrano E, Coma R, Inostroza K, Serrano O. Polyp bail-out by the coral *Astroides calycularis* (*Scleractinia, Dendrophylliidae*). *Mar Biodiv*. 2018;48(3):1661-1665.

   doi: 10.1007/s12526-017-0647-x

5. Cardoso PM, Alsaggaf AA, Villela HM, Peixoto RS. Inducing polyp bail-out in coral colonies to obtain individualized micropropagates for laboratory experimental use. *J Vis Exp.* 2022;(182):63840.

   doi: 10.3791/63840

6. Shapiro OH, Kramarsky-Winter E, Gavish AR, Stocker R, Vardi A. A coral-on-a-chip microfluidic platform enabling live-imaging microscopy of reef-building corals. *Nat Commun.* 2016;7(1):10860.

   doi: 10.1038/ncomms10860

7. Pang AP, Luo Y, He C, Lu Z, Lu X. A polyp-on-chip for coral long-term culture. *Sci Rep.* 2020;10(1):6964.

   doi: 10.1038/s41598-020-63829-4

8. Chuang PS, Ishikawa K, Mitarai S. Morphological and genetic recovery of coral polyps after bail-out. Front Mar Sci. 2021;8:609287.

   doi: 10.3389/fmars.2021.609287

9. Hauser CAE, Deng R, Mishra A, *et al*. Natural tri- to hexapeptides self-assemble in water to amyloid β-type fiber aggregates by unexpected α-helical intermediate structures. *Proc Natl Acad Sci USA*. 2011;108(4):1361-1366.

   doi: 10.1073/pnas.1014796108

10. Roger LM, Lewinski NA, Putnam HM, Roxbury D, Tresguerres M, Wangpraseurt D. Nanobiotech engineering for future coral reefs. *One Earth.* 2023;6(7):778-789.

    doi: 10.1016/j.oneear.2023.05.008

11. Susapto HH, Alhattab D, Abdelrahman S, *et al.* Ultrashort peptide bioinks support automated printing of large-scale

constructs assuring long-term survival of printed tissue constructs. *Nano Lett*. 2021;21(7):2719-2729.

doi: 10.1021/acs.nanolett.0c04426

12. Tóth GS, Backman O, Siivola T, *et al.* Employing photocurable biopolymers to engineer photosynthetic 3D-printed living materials for production of chemicals. *Green Chem*. 2024;26(7):4032-4042.

doi: 10.1039/D3GC04264B

13. Wangpraseurt D, You S, Azam F, *et al*. Bionic 3D printed corals. *Nat Commun*. 2020;11(1):1748.

doi: 10.1038/s41467-020-15486-4

14. Wangpraseurt D, Sun Y, You S, *et al*. Bioprinted living coral microenvironments mimicking coral-algal symbiosis. *Adv Funct Mater*. 2022;32(35):2202273.

doi: 10.1002/adfm.202202273

15. Roger L, Lewinski N, Putnam H, *et al.* Nanotechnology for coral reef conservation, restoration and rehabilitation. *Nat Nanotechnol*. 2023;18(8):831-833.

doi: 10.1038/s41565-023-01402-6

16. de León EHP, Valle-Pérez AU, Khan ZN, Hauser CAE. Intelligent and smart biomaterials for sustainable 3D printing applications. *Curr Opin Biomed Eng*. 2023;26:100450.

doi: 10.1016/j.cobme.2023.100450

17. Zhao S, Guo C, Kumarasena A, Omenetto FG, Kaplan DL. 3D printing of functional microalgal silk structures for environmental applications. *ACS Biomater Sci Eng.* 2019;5(9):4808-4816.

doi: 10.1021/acsbiomaterials.9b00554

18. Krujatz F, Lode A, Brüggemeier S, *et al*. Green bioprinting: Viability and growth analysis of microalgae immobilized in 3D-plotted hydrogels versus suspension cultures. *Eng Life Sci*. 2015;15(7):678-688.

doi: 10.1002/elsc.201400131

19. Wangpraseurt D, You S, Sun Y, Chen S. Biomimetic 3D living materials powered by microorganisms. *Trends Biotechnol*. 2022;40(7):843-857.

doi: 10.1016/j.tibtech.2022.01.003

20. Valenzuela Matus I, Góis J, Vaz-Pires P, Lino Alves J. Coral propagation in substrates obtained through additive manufacturing: Influence of mortar formulations on seawater parameters. *ACS Sustain Chem Eng.* 2024;12(37):13721-13740.

doi: 10.1021/acssuschemeng.4c01276

21. Levy N, Kundu S, Freckelton M, *et al.* Microbial living materials promote coral larval settlement. PNAS Nexus. 2025;4(9):pgaf268.

doi: 10.1093/pnasnexus/pgaf268

22. Contardi M, Fadda M, Isa V, *et al*. Biodegradable Zein-based biocomposite films for underwater delivery of curcumin reduce thermal stress effects in corals. *ACS Appl Mater Interfaces*. 2023;15(28):33916-33931.

doi: 10.1021/acsami.3c01166

23. Luo C, Li M, Yuan R, Yang Y, Lu Z, Ge L. Biocompatible self-healing coating based on schiff base for promoting adhesion of coral cells. *ACS Appl Bio Mater*. 2020;3(3):1481-1495.

doi: 10.1021/acsabm.9b01113

24. Roger LM, Adarkwa Darko Y, Bernas T, *et al.* Evaluation of fluorescence-based viability stains in cells dissociated from scleractinian coral *Pocillopora damicornis*. *Sci Rep.* 2022;12(1):15297.

doi: 10.1038/s41598-022-19586-7

25. Baker NR. Chlorophyll fluorescence: A probe of photosynthesis *in vivo*. *Annu Rev Plant Biol.* 2008;59(1):89-113.

doi: 10.1146/annurev.arplant.59.032607.092759

26. Overmans S, Ignacz G, Beke AK, *et al*. Continuous extraction and concentration of secreted metabolites from engineered microbes using membrane technology. *Green Chem.* 2022;24(14):5479-5489.

doi: 10.1039/D2GC00938B

27. Khan Z, Kahin K, Hauser C. Time-dependent pulsing of microfluidic pumps to enhance 3D bioprinting of peptide bioinks. In: Gray BL, Becker H, editors. *Microfluidics, BioMEMS, and Medical Microsystems XIX*. Washington, DC: SPIE; 2021. p. 5.

doi: 10.1117/12.2578830

28. Rauf S, Susapto HH, Kahin K, *et al*. Self-assembling tetrameric peptides allow in situ 3D bioprinting under physiological conditions. *J Mater Chem B.* 2021;9(4): 1069-1081.

doi: 10.1039/D0TB02424D

29. Unal AZ, West JL. Synthetic ECM: Bioactive synthetic hydrogels for 3D tissue engineering. *Bioconjugate Chem.* 2020;31(10):2253-2271.

doi: 10.1021/acs.bioconjchem.0c00270

30. Bilalis P, Alrashoudi AA, Susapto HH, *et al*. Dipeptide-based photoreactive instant glue for environmental and biomedical applications. *ACS Appl Mater Interfaces*. 2023;15(40): 46710-46720.

doi: 10.1021/acsami.3c10726

31. Jia Y, Abdelrahman S, Hauser CAE. Developing a sustainable resin for 3D printing in coral restoration. *MSAM*. 2024;3(2):3125.

doi: 10.36922/msam.3125

32. Albalawi HI, Khan ZN, Valle-Pérez AU, *et al.* Sustainable

and eco-friendly coral restoration through 3D printing and fabrication. *ACS Sustain Chem Eng*. 2021;9(37): 12634-12645.

doi: 10.1021/acssuschemeng.1c04148

33. Do TD, LaPointe NE, Economou NJ, *et al.* Effects of pH and charge state on peptide assembly: The YVIFL model system. *J Phys Chem B*. 2013;117(37):10759-10768.

doi: 10.1021/jp406066d

34. Hopkins E, Sanvictores T, Sharma S. *Physiology, Acid Base Balance*. Treasure Island, FL: StatPearls Publishing; 2024.

35. Abdelmongy A, El-Moselhy K. Seasonal variations of the physical and chemical properties of seawater at the Northern Red Sea, Egypt. *Open J Ocean Coastal Sci*. 2015;2(1):1-17.

doi: 10.15764/OCS.2015.01001

36. Rasul NMA, Stewart ICF, editors. *Oceanographic and Biological Aspects of the Red Sea.* Berlin: Springer International Publishing; 2019.

doi: 10.1007/978-3-319-99417-8

37. Hauser CAE, Zhang S. Designer self-assembling peptide nanofiber biological materials. *Chem Soc Rev*. 2010;39(8):2780.

doi: 10.1039/b921448h

38. Zhao X, Pan F, Xu H, *et al*. Molecular self-assembly and applications of designer peptide amphiphiles. *Chem Soc Rev*. 2010;39(9):3480.

doi: 10.1039/b915923c

39. Chan KH, Lee WH, Ni M, Loo Y, Hauser CAE. C-terminal residue of ultrashort peptides impacts on molecular self-assembly, hydrogelation, and interaction with small-molecule drugs. *Sci Rep.* 2018;8(1):17127.

doi: 10.1038/s41598-018-35431-2

40. Haerianardakani S, Kreutzer AG, Salveson PJ, Samdin TD, Guaglianone GE, Nowick JS. Phenylalanine mutation to cyclohexylalanine facilitates triangular trimer formation by β-hairpins derived from Aβ. *J Am Chem Soc*. 2020;142(49):20708-20716.

doi: 10.1021/jacs.0c09281

41. Brower DL, Brower SM, Hayward DC, Ball EE. Molecular evolution of integrins: Genes encoding integrin β subunits from a coral and a sponge. *Proc Natl Acad Sci USA*. 1997;94(17):9182-9187.

doi: 10.1073/pnas.94.17.9182

42. Iguchi A, Márquez LM, Knack B, *et al.* Apparent involvement of a β1 type integrin in coral fertilization. *Mar Biotechnol*. 2007;9(6):760-765.

doi: 10.1007/s10126-007-9026-0

43. Jones VAS, Dorr M, Siemers I, *et al*. Symbiont-specific uptake is mediated by integrins in cnidarian larvae. bioRxiv. 2025.

doi: 10.1101/2025.01.21.633834

44. Levy S, Elek A, Grau-Bové X, *et al*. A stony coral cell atlas illuminates the molecular and cellular basis of coral symbiosis, calcification, and immunity. *Cell*. 2021; 184(11):2973-2987.e18.

doi: 10.1016/j.cell.2021.04.005

45. Mao X, Nie Y, Huang Y, Ji H, Li X. A radial distribution of calices in coral skeleton of *Pocillopora verrucosa* (Ellis and Solander, 1786) against ocean currents. *Mar Biol.* 2021;168(12):171.

doi: 10.1007/s00227-021-03982-0

46. Xu J, Pérez-Pedroza R, Moretti M, *et al*. 3D bioprinting of colon organoids in ultrashort self-assembling and decorated peptide matrices. *IJB*. 2024;0(0):3033.

doi: 10.36922/ijb.3033

47. Su T, Liu Y, He H, *et al*. Strong bioinspired polymer hydrogel with tunable stiffness and toughness for mimicking the extracellular matrix. *ACS Macro Lett*. 2016;5(11):1217-1221.

doi: 10.1021/acsmacrolett.6b00702

48. Trappmann B, Chen CS. How cells sense extracellular matrix stiffness: A material's perspective. *Curr Opin Biotechnol*. 2013;24(5):948-953.

doi: 10.1016/j.copbio.2013.03.020

49. Wen JH, Vincent LG, Fuhrmann A, *et al*. Interplay of matrix stiffness and protein tethering in stem cell differentiation. *Nat Mater*. 2014;13(10):979-987.

doi: 10.1038/nmat4051

50. Wiedenmann J, D'Angelo C, Mardones ML, *et al*. Reef-building corals farm and feed on their photosynthetic symbionts. *Nature*. 2023;620(7976):1018-1024.

doi: 10.1038/s41586-023-06442-5

51. Weis VM. Corals have algal friends for dinner. *Nature*. 2023;620(7976):951-952.

doi: 10.1038/d41586-023-02593-7

52. Avila-Ramírez A, Valle-Pérez AU, Susapto HH, *et al*. Ecologically friendly biofunctional ink for reconstruction of rigid living systems under wet conditions. *Int J Bioprint*. 2021;7(4):398.

doi: 10.18063/ijb.v7i4.398